

Optimization of experimental parameters of laser induced soil plasma spectral radiation

Wang Jinmei, Yan Haiying, Zheng Peichao*, Xue Shuwen

(Chongqing Municipal Level Key Laboratory of Photoelectronic Information Sensing and Transmitting Technology, College of Optoelectronic Engineering, Chongqing University of Posts and Telecommunications, Chongqing 400065, China)

Abstract: Laser induced breakdown spectroscopy (LIBS) was employed to investigate the soil. LIBS analyses were performed with Nd: YAG laser operating at 1 064 nm, 5.82 ns pulse duration. The spectral lines of Ca II 393.37 nm and Ca II 396.85 nm were selected as the analytical lines for optimizing the experimental parameters (ICCD delay, laser energy, ICCD gate width, repetition rate and cumulative number of spectrum) which had influence on spectral line. The experimental conditions were determined as follows. The ICCD delay was 1 μs , the laser energy was 50 mJ, the ICCD gate width was 3.5 μs , the repetition rate was 1 Hz and the cumulative number of spectrum was 100 times. Under the optimal experimental conditions, the results of the electron temperatures T_e and electron densities N_e were 11 604 K and $5.155 \times 10^{16} \text{ cm}^{-3}$, respectively. The local thermal equilibrium condition of the plasma was satisfied. The results are useful for the analysis and detection of elements in soil.

Key words: laser induced breakdown spectroscopy; sequential test; soil; electron temperatures; electron densities

CLC number: O433.4; TN249 **Document code:** A **DOI:** 10.3788/IRLA201847.1206011

激光诱导土壤等离子体光谱辐射实验参数优化

王金梅, 颜海英, 郑培超*, 薛淑文

(重庆邮电大学 光电工程学院 光电信息感测与传输技术重庆重点实验室, 重庆 400065)

摘要: 采用激光诱导击穿光谱法(LIBS)对土壤进行了研究。激光器采用的是 Nd: YAG 脉冲激光器, 激光器的输出波长是 1 064 nm, 脉宽是 5.82 ns, 激光聚焦在土壤表面产生激光诱导等离子体, 通过优化实验参数(ICCD 延时、脉冲能量、ICCD 门宽、脉冲频率、谱图积累次数)对 Ca II 393.37 nm 和 Ca II 396.37 nm 两条特征谱线强度及信背比的影响, 确定实验最佳条件是 ICCD 延时 1 μs , 激光能量 50 mJ, ICCD 门宽 3.5 μs , 脉冲频率 1 Hz, 谱图积累次数 100 次。在最优实验条件下计算等离子体参数, 得出土壤中的等离子体电子温度是 11 604 K, 土壤的等离子体电子密度是 $5.155 \times 10^{16} \text{ cm}^{-3}$, 经过

收稿日期: 2018-07-10; 修订日期: 2018-08-28

基金项目: 重庆市基础科学与前沿技术研究专项项目重点项目(cstc2015jcyjBX0016); 重庆市教委科学研究项目(KJ1500436); 教育部留学回国人员科研启动基金(教外司留[2015]1098号); 重庆市基础科学与前沿技术研究专项项目一般项目(cstc2016jcyjA0389); 重庆邮电大学博士基金(A2016-113)

作者简介: 王金梅(1981-), 女, 副教授, 博士, 主要从事光电检测技术方面的研究。Email: wangjm@cqupt.edu.cn

通讯作者: 郑培超(1980-), 男, 教授, 博士, 主要从事光谱测量技术方面的研究。Email: zhengpc@cqupt.edu.cn

计算,土壤样品满足 LTE 条件。这说明,以上关于土壤样品的等离子体参数计算结果是真实有效的。

关键词: 激光诱导击穿光谱; 序贯试验法; 土壤; 电子温度; 电子密度

0 Introduction

It is well known that an agricultural producer may encounter with a variety of soil types due to non-uniform distribution of nutrients. Due to it, the field may result in over use of nutrients and could embrace inefficient allocation of resources. Over fertilization is dangerous and may even lead to environmental problems, such as greenhouse farm downtime, affect the water level. Precision farming and management of nutrients allows growers to optimize input of nutrients specially, Calcium, Phosphorus, Nitrogen, Sulfur, Iron and Potassium, on a site-specific basis. It is necessary to identify nutrient elements and trace elements in the soil, which is benefit for accurately analyzing soil fertility, reducing agricultural cost and environmental pollution.

The common analytical methods, such as Inductively Coupled Plasma-Optical Emission Spectroscopy (ICP-OES), Inductively Coupled Plasma-Mass Spectroscopy (ICP-MS), and Atomic Absorbance Spectroscopy (AAS), are used to determine element concentrations in soil. These analytical methods require time consuming, costly collection and pre-treatment of samples prior to analysis^[1]. Compared with conventional elemental analytical methods, LIBS has numerous potential advantages^[2].

Laser induced breakdown spectroscopy was proposed by Brech F and Cross L in 1962 as a new method for material element detection. Due to its advantages such as negligible sample pre-treatment, high sensitivity, real-time response, simultaneous multi-elemental detection of major and trace element^[3-4], it has broad application prospects in the archaeological, exploration, metallurgy and other fields^[5-6]. The results of

LIBS technology applied to soil nutrient testing have been reported, mainly focusing on the analysis of total element concentration of total carbon, inorganic carbon, total nitrogen, total phosphorus and total potassium in soil. Ayyalasomayajula K K et al.^[7] analyzed the total carbon concentration in soil by LIBS. Martin M Z et al.^[8] studied the detection of total carbon, inorganic carbon and organic carbon in soil. Meng D^[9] reported the determination of total potassium in the soil.

The impacts of the ICCD delay, laser energy, ICCD gate width, laser repetition rate and cumulative number of spectrum on the spectral line cannot be ignored. In this paper, the sequential test method is used to optimize the ICCD delay, laser energy, ICCD gate width, laser repetition rate and the cumulative number of spectrum. The sequential test is a method of planning and arranging subsequent tests based on the previous test effect. Thus, optimal experimental conditions can be obtained. Under these optimal experimental conditions, the temperature T_e and electron density N_e of the plasma can be calculated. The optimization of these parameters is helpful for further qualitative and quantitative analysis of soil.

1 Experiment

A schematic view of the experimental set-up is presented in Fig.1. A Q-switched Nd: YAG laser (Big Sky Laser Technology, Ultra 100), at a fundamental wavelength of 1 064 nm with a pulse duration of 5.82 ns, a repetition rate of 20 Hz and a maximum pulse energy of 100 mJ, was used as the excitation laser. The energy of the laser could be adjusted by changing the Q delay time, and evaluated by using an optical power meter. The laser

beam was focused perpendicularly to the surface of the sample on a two-dimensional translation stage, which was controlled by a controller (Zolix SC300-2A) with a plano-convex lens ($f=100$ mm) to produce an intense, transient plasma. The emission from the plasma was collected by a two plano-convex lenses and a 2 m long multimode silica fiber. The light was then transmitted through the fiber to the entrance of a computerized Czerny-Turner spectrograph (Andor Model SR-750 A). The spectrograph equipped with three ruled gratings, 2 400 grooves/mm, 1 200 grooves/mm and 300 grooves/mm, which were interchangeable under computer control, providing high and low resolution spectra in the wavelength range 200-900 nm. A gated and intensified CCD (ICCD) camera (Andor DH340T-18U-03) was coupled to the output end of the spectrograph. The ICCD camera had 2 048 pixel \times 512 pixel and was cooled to -15 $^{\circ}$ C by a Peltier cooler to reduce noise.

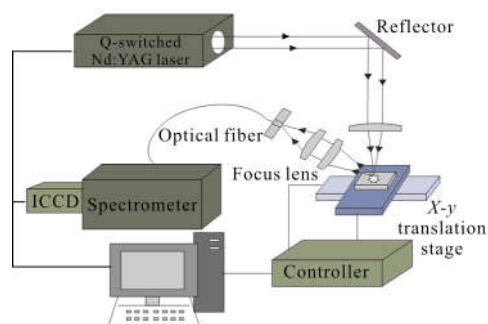


Fig.1 Schematic of the experimental LIBS setup

The soil was taken from the campus of Chongqing University of Posts and Telecommunications. The soil was naturally dried, removed the impurities, and crushed to powders. The sifted soil powders were pressed into tablets with 2 mm thickness, 15 mm diameter using a hydraulic tablet machine.

Twenty laser pulses were accumulated to obtain each spectrum, and each experimental condition that was analysed using LIBS was the

average of ten spectrum measurements, in order to increase the sensitivity and reduce the standard deviation.

2 Results and discussion

Figure 2 shows the LIBS spectra of the soil with wavelengths from 370 nm to 400 nm. The spectral lines of metallic elements such as Mg, Si, Ca and Al are shown. The spectral lines of Ca II 393.37 nm and Ca II 396.85 nm in the soil sample are studied.

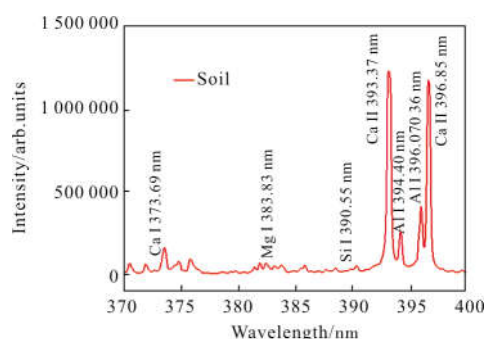


Fig.2 LIBS spectra of soil

2.1 Influence of ICCD delay on spectral signal

Figure 3 presents the intensity and signal background ratio (SBR) evolution of the spectral lines as the ICCD delay was varied from 0.1 μ s to 24 μ s, when the laser energy is 25 mJ, the ICCD gate width is 0.5 μ s and the repetition rate is 4 Hz.

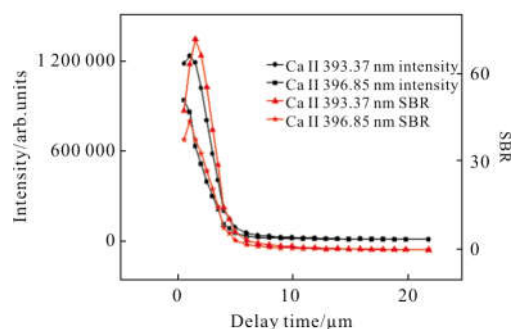


Fig.3 Ca II 393.37 nm and Ca II 396.85 nm spectral line strength and SBR as the ICCD delay time changes

In the first step, the laser energy is absorbed by the sample surface, and particles are motivated from the soil sample, in the second step, initial

products ablated by the laser form stronger plasma, and in the third step, after transiting to a low-level, atoms and ions in the low-level state form a characteristic line, then the plasma is extinguished. As can be seen in Fig.3, the spectral intensities of the two lines of Ca firstly increase and then rapidly decrease with the ICCD delay time increasing. The maximum spectral intensities of the Ca II 393.37 nm line and the Ca II 396.85 nm line are observed at 1.5 μ s and 1 μ s, respectively. When the delay time is more than 5 μ s, the plasma is almost extinguished. The SBR decreases rapidly after a little increase. The maximum SBR of Ca II 393.37 nm and Ca II 396.85 nm are observed at 1 μ s. The background signal is very strong at the beginning, and then decreases rapidly after 1 μ s. Therefore, the SBR increases gradually at the beginning of the plasma formation, then decreases with the reduction of the spectral signal. The signal intensities and SBR of the two lines are analysed synthetically, and then 1 μ s is taken as the best delay time.

2.2 Influences of laser energy on the spectral signals

Figure 4 presents the intensity and SBR evolution of the CaII spectral lines as the laser energy varied from 1 mJ to 100 mJ, when the ICCD delay is 1 μ s, the ICCD gate width is 2 μ s and the repetition rate is 4 Hz.

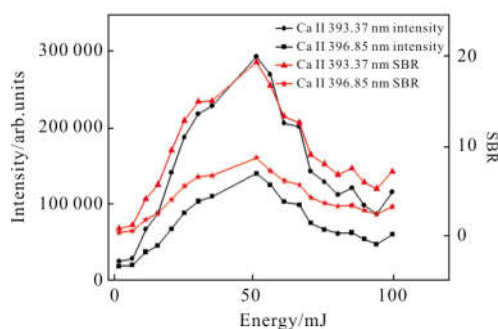


Fig.4 Ca II 393.37 nm and Ca II 396.85 nm spectral line strength and SBR as the laser energy changes

In the laser ablation process, the plasma is

produced when the laser energy exceeds its the threshold of the plasma ignition. As shown in Fig.4, when the laser energy is low, as the laser energy increases, the soil sample is ablated more, the intensities and SBR of Ca II 393.37 nm and Ca II 396.85 nm increase. Higher laser energies produces stronger ablations, and higher intensities of the spectral lines are obtained at higher laser energies. As the laser energy gets higher than 50 mJ, the intensities of the spectral lines decrease. Excessively high laser energy destroys the samples and creates a much larger ablation crater. In addition, a larger amount of powder is produced above the sample, which decreases the intensities, stabilizes the spectral lines, and causes higher standard deviations. Therefore, the optimal laser energy is 50 mJ.

2.3 Influences of the ICCD gate width on the spectral signals

Figure 5 presents the intensity and SBR evolution of the spectral lines as the gate width varies from 0.1 μ s to 20 μ s, when the ICCD delay is 1 μ s, and the laser energy is 50 mJ and the repetition rate is 4 Hz.

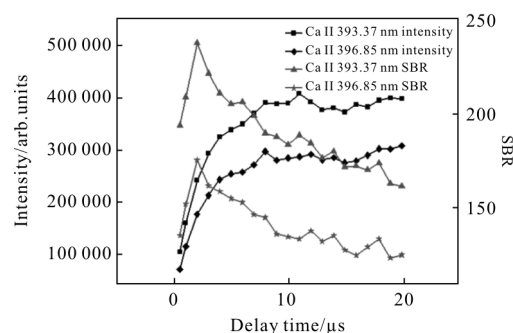


Fig.5 Ca II 393.37 nm and Ca II 396.85 nm spectral line strength and SBR as the ICCD gate width changes

The ICCD gate width refers to the length of the signal acquisition time. Figure 5 shows that when the ICCD gate width is in the range of 0–8 μ s, Ca II 393.37 nm and Ca II 396.85 nm line intensities increase rapidly as the ICCD gate width increases. When the delay time is more than 8 μ s,

the spectral intensities tend to be gentle. SBR increase linearly up as the ICCD gate width increase and then decrease after 2 μs . The background signal reduces rapidly shortly after ablation. Taking the intensities and SBR into account, the optimal ICCD gate width is 3.5 μs .

2.4 Influence of laser pulse frequency on the spectral signals

Figure 6 presents the intensity and relative standard deviation (RSD) evolution of these spectral lines as the laser pulse frequency is varied from 0.5 Hz to 20 Hz, when the laser energy is 50 mJ, the ICCD delay is 1 μs and the ICCD gate width is 3.5 μs .

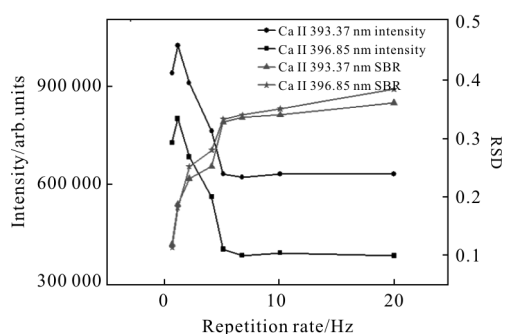


Fig.6 Ca II 393.37 nm and Ca II 396.85 nm spectral line strength and RSD as the laser repetition rate changes

The laser repetition rate has an effect on the intensity and RSD of the spectrum^[10], it shows that the spectral intensities of the two lines of Ca increase firstly and then decrease rapidly. At 0.5 Hz to 1 Hz, the line rises because the greater the impact of external interference received when the repetition rate is low. Range 1–5 Hz, the line decreases greatly. The laser ablates the sample and leaving the ablated pits, ablated dust will be the excitation point, and it will not dissipate in a short period of time. The repetition rate at a high level, this dust is not conducive to the spectrometer detection.

As the repetition rate increases, the RSD of the spectral lines also increases. The higher the laser repetition frequency is, the more unstable the

laser energy is, while the dust will cause the collection spectrum error. Therefore, the lower the repetition rate received, the smaller the RSD is. Taking the intensities and RSD into account, the optimal repetition rate is 1 Hz.

2.5 Influence of cumulative number of spectrum on RSD

Figure 7 presents the RSD evolution of these spectral lines as the cumulative number of spectrum is varied from 10 times to 220 times, when the laser energy is 50 mJ, the ICCD delay is 1 μs , the ICCD gate width is 3.5 μs and repetition rate is 1 Hz.

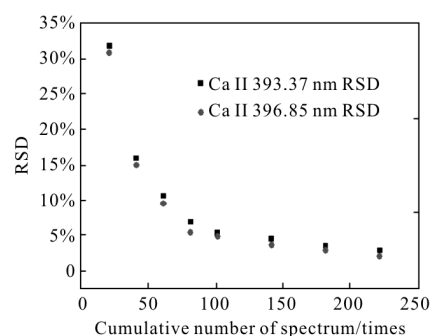


Fig.7 Ca II 393.37 nm and Ca II 396.85 nm spectral line RSD as the cumulative number of spectrum changes

This part tests the relationship between RSD and the cumulative number of spectrum. As can be seen from Fig.7, the RSD becomes lower as the number of times increases. If a sufficient number of the accumulation is used, the RSD can be reduced to 2%. Taking into account the experimental efficiency, the cumulative number of spectrum is 100 times.

2.6 Plasma temperature of the soil

The Boltzmann oblique line method is used to calculate the electron temperature of plasma in this experiment. The plasma parameters, including electron temperature T_e and electron number density N_e , are essential for the LIBS technique. The calculation of plasma temperature and electron density should satisfy the assumption of

local thermodynamic equilibrium (LTE). The following relation is used to extract the electron temperature^[11]:

$$\ln\left(\frac{I_{ki}\lambda_{ki}}{A_{ki}g_k}\right) = -\frac{E_k}{k_B T_e} + a \quad (1)$$

Where λ_{ki} is the known constant, k_B is the Boltzmann constant, A_{ki} is the transition probability, and I_{ki} is the spectral intensity of the corresponding spectrum. Statistical weight g_k and the upper-level

energy E_k can be found in the NIST database. In these experiments, the spectral lines of Ca II 317.93 nm, Ca II 370.60 nm, Ca II 373.69 nm, Ca II 393.37 nm and Ca II 396.85 nm of the same ionization order for the same element were used to calculate the electron temperature. The spectral parameters of the five Ca II line are shown in Tab.1.

Linear fitting is performed using Origin

Tab.1 Spectral parameters of Ca II emissions used for the Boltzmann oblique line method

Wavelength λ /nm	Transition parameters	Statistical weight g_k	Transition probability $A_{ki}(s-1)$	Energy level/eV	
				E_k	E_i
317.93	$3p^6 4d^2 D_{3/2} \rightarrow 3p^6 4p^2 P_{1/2}^0$	6	3.6×10^8	7.049 1	3.150 98
370.60	$3p^6 5s^2 S_{1/2} \rightarrow 3p^6 4p^2 P_{1/2}^0$	2	8.8×10^8	6.467 8	3.123 34
373.69	$3p^6 5s^2 S_{1/2} \rightarrow 3p^6 4p^2 P_{3/2}^0$	2	1.7×10^8	6.46 78	3.150 98
393.37	$3p^6 4p^2 P_{3/2}^0 \rightarrow 3p^6 4s^2 S_{1/2}$	4	1.47×10^8	3.150 9	0
396.85	$3p^6 4p^2 P_{1/2}^0 \rightarrow 3p^6 4s^2 S_{1/2}$	2	1.4×10^8	3.123 3	0

software, and the results are shown in Fig.8. The electron temperature is 11 604 K.

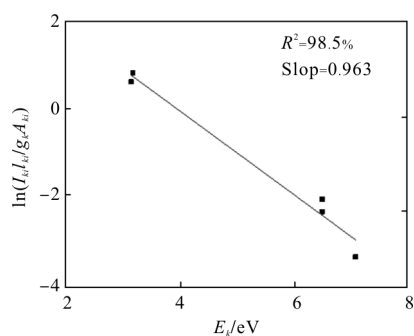


Fig.8 Boltzmann linear fitting of Ca II line in soil

The movement of electrons is the largest source of energy exchange in the laser induced plasma plume. Therefore, the plasma electron density has a significant effect on the LIBS plasma performance analysis. The electron number density N_e of the plasma in the soil can be calculated using the following formula^[11]:

$$\Delta\lambda_{1/2} = 2\omega \left(\frac{N_e}{10^{16}} \right) \quad (2)$$

Where ω is the electron impact width parameter, N_e is the electron number density, and $\Delta\lambda_{1/2}$ can

be obtained by Lorentz fitting of the source line by Origin software. Choosing Ca II 393.37 nm as the fitting object spectrum, the Lorentz fitting curve is shown in Fig.9. FWHM can be deduced from the half width of Fig.9. The soil sample has electron number density $5.155 \times 10^{16} \text{ cm}^{-3}$.

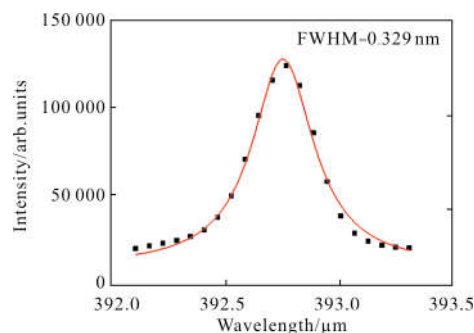


Fig.9 Lorentz fitting of Stark broadening of Ca II 393.37 nm in soil

In this work, there is no dip at the central frequency of the emission lines. So it is assumed from experiment that the plasma can be described by local thermodynamic equilibrium (LTE). The necessary condition for LTE that gives the corresponding lower limit of the electron number

density N_e is given by the McWhirter criterion^[11]:

$$N_e \geq 1.6 \times 10^{12} T_e^{1/2} (\Delta E)^3 \quad (3)$$

Where ΔE is the highest energy transition for which the condition holds. In the experiments, the soil sample exhibits electron temperature of 11 604 K and $\Delta E=3.8986$ eV. The electron number density is $5.155 \times 10^{16} \text{ cm}^{-3}$. Therefore, the condition for LTE was fulfilled for the laser-induced plasma in our experiment.

3 Conclusion

In this paper, it is found that the ICCD time delay, the laser energy, the ICCD gate width, the repetition rate and the cumulative number of spectrum have great influences on the LIBS signals. When the ICCD delay is 1 μs , the laser energy is 50 mJ, the ICCD gate width is 3.5 μs and the repetition rate is 1 Hz, the cumulative number of spectrum is 100 times, the detection accuracy can be improved and the optimal LIBS spectra are obtained. In addition, under the optimal conditions for soil LIBS experiment, the plasma parameters (electron temperature and electron number density) are 11 604 K and $5.155 \times 10^{16} \text{ cm}^{-3}$, and the LTE are satisfied. This indicates that the calculated results for the plasma parameters for soil samples are real and effective.

References:

[1] Li Zhanfeng, Wang Ruiwen, Deng Hu, et al. Laser induced breakdown spectroscopy of Pb in *Coptis chinensis* [J]. *Infrared and Laser Engineering*, 2016, 45(10): 1006003. (in Chinese)
李占锋, 王芮雯, 邓琥, 等. 黄连中 Pb 的激光诱导击穿光谱测量分析[J]. *红外与激光工程*, 2016, 45(10): 1006003.

[2] Senesi G S, Senesi N. Laser-induced breakdown spectroscopy (LIBS) to measure quantitatively soil

carbon with emphasis on soil organic carbon. A review [J]. *Analytica Chimica Acta*, 2016, 938: 7–17.

[3] Pandey S, Martinez M, Hosta J, et al. Quantification of SiO₂ sintering additive in YAG transparent ceramics by laser-induced breakdown spectroscopy (LIBS) [J]. *Opt Mater Express*, 2017, 7(5): 1666–1671.

[4] Noll R, Sturm V, Ümit Aydin, et al. Laser-induced breakdown spectroscopy—From research to industry, new frontiers for process control [J]. *Spectrochimica Acta Part B Atomic Spectroscopy*, 2008, 63(10): 1159–1166.

[5] Anderson D E, Ehlmann B L, Forni O, et al. Characterization of LIBS emission lines for the identification of chlorides, carbonates, and sulfates in salt/basalt mixtures for the application to MSL ChemCam data [J]. *Journal of Geophysical Research Planets*, 2017, 122: 744–770.

[6] Wang J, Shi M, Zheng P, et al. Quantitative analysis of lead in tea samples by laser-induced breakdown spectroscopy [J]. *Journal of Applied Spectroscopy*, 2017, 84(1): 188–193.

[7] Ayyalasomayajula K K, Yu-Yueh F, Singh J P, et al. Application of laser-induced breakdown spectroscopy for total carbon quantification in soil samples. [J]. *Applied Optics*, 2012, 51(7): 149–54.

[8] Martin M Z, Mayes M A, Heal K R, et al. Investigation of laser-induced breakdown spectroscopy and multivariate analysis for differentiating inorganic and organic C in a variety of soils [J]. *Spectrochimica Acta Part B Atomic Spectroscopy*, 2013, 87(9): 100–107.

[9] Meng D, Zhao N, Liu W, et al. Study on removing method of continuous background spectrum in LIBS of multi-element heavy metals in water [J]. *Chinese Journal of Lasers*, 2014, 41(7): 0715003. (in Chinese)

[10] Lu C, Liu W, Zhao N, et al. Quantitative analysis of chrome in soil samples using laser-induced breakdown spectroscopy [J]. *Acta Physica Sinica*, 2011, 60(4): 388–392. (in Chinese)

[11] Zheng P, Shi M, Wang J, et al. The spectral emission characteristics of laser induced plasma on tea samples [J]. *Plasma Science Technology*, 2015, 17(8): 664–670.